Thermal Impact Analysis of Circulating Current in High Power Modular Online Uninterruptible Power Supplies Application

Zhang, Chi; Guerrero, Josep M.; Vasquez, Juan Carlos

Published in:
Proceedings of the 17th Conference on Power Electronics and Applications, EPE'15-ECCE Europe

DOI (link to publication from Publisher):
10.1109/EPE.2015.7311739

Publication date:
2015

Document Version
Early version, also known as pre-print

Thermal Impact Analysis of Circulating Current in High Power Modular Online Uninterruptible Power Supplies Application

Chi Zhang, Josep M. Guerrero, Juan C. Vasquez
Aalborg University
Pontoppidanstraede 101
Aalborg, Denmark
Tel.: +45 / 30553329
E-Mail: zhc@et.aau.dk, joz@et.aau.dk, juq@et.aau.dk
URL: http://www.microgrids.et.aau.dk/

Keywords

Modular UPS system, zero sequence circulating current, thermal analysis.

Abstract

In a modular uninterruptible power supplies (UPS), each DC/AC module was designed to work in a circular way considering the reliability and power stress issues of the whole system. Thus unsynchronized PWMs will occur if any of the DC/AC modules is plugged in or out of the system at any time. On the other hand, modular difference is another issue that will bring such kind of circulating current. In order to reduce system size and cost, each module shares the same DC and AC bus without any isolation or passive elements in the system. Consequently, potential zero-sequence current is possible to occur and should be paid specific attention. In this paper, a four-module online UPS system is designed. And thermal and loss distribution condition are investigated under different circulating current condition with conventional three phase H-bridge topology.

Introduction

During the past decades, power quality issues are receiving more and more attention from both academic and industrial field due to the prosperity for a large amount of advanced electrical load, for instance, IT equipment, medical facilities and so on [1]. This puts huge challenge for the utility. At the same time, the utility is becoming weak due to boom of the renewable energy and distributed generation system. It is easy to be blackout since solar energy or wind energy is unpredictable [2]. As a result, UPS system, as a one of the most commercialized power electronics equipment, is developing fast as an energy supporter in case of any emergency during the past decades.

Compared with offline and line-interactive UPS system, online UPS system, also named inverter preferred or double conversion UPS, mainly aims at high power application due to its output voltage controllability and its decoupling capability of the utility and the load [3], [4]. For the sake of system flexibility and expansibility, a series of different modular UPS system structure is proposed in [5]-[7]. Normally, a number of DC/AC modules are used to work in parallel together as the inverter stage as shown in Fig. 1(a).

It can be observed that all DC/AC modules share the same DC bus and AC bus with not galvanic isolation. Such kind of structure provides the possible flowing path for zero sequence current [8]-[11] due to mismatched physical parameters, different control parameters, unsynchronized PWM and so on. Much research has been done in order to suppress or reduce such a kind of zero-sequence circulating currents. In general, four kinds of techniques can be found: isolation [8], high impedance [9], synchronized control [10], and active suppression [11], are used to eliminate such a kind of circulating current.

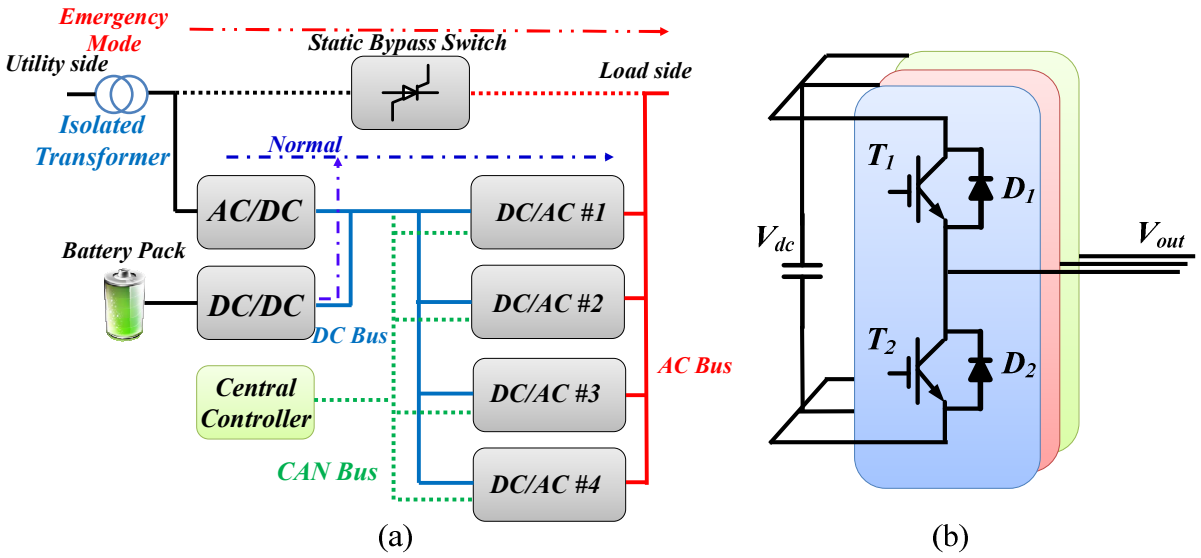

Fig. 1: Modular online UPS system. (a) system structure; (b) Converter topology.

In order to have all the DC/AC modules share the same active and reactive power, various kinds of parallel technology have been proposed [12]-[15]. These control methods concentrates on modifying UPS system output voltage amplitude, frequency or phase. Consequently, UPS output voltage becomes load dependent. Voltage amplitude and frequency are fluctuant in different load condition. So with communication network, a higher level controller, namely recovery control, is proposed to maintain the UPS output voltage stable [16], [17] since mature DSP technology provides a much smaller communication delay for CAN bus [18]. However, these methods aren't able to suppress the zero sequence circulating current. It still has negative impacts on losses and thermal distribution of the devices in the hardware circuit. The unbalanced losses and thermal distribution performances, especially in high power modular scenarios, are also required to be investigated further, which can be a guide concerning heat problems in designing the modular online UPS systems.

In this paper, a modular structure is implemented with four DC/AC inverters operating in parallel, as shown in Fig. 1(a). Conventional H-bridge topology (see Fig. 1(b)) is considered in this application, and the four modules are designated to work in a circular way to make sure that each module can have balanced thermal and loss conditions. Such a kind of *plug'n'play* system will result in unsynchronized PWMs as well as module difference, which will cause zero sequence circulating current. Based on the thermal model proposed in [19], different circulating current scenarios are simulated in PLECS to evaluate its impact on thermal losses of the devices in each module by evaluating the devices thermal models, which can be found in the manufacturer datasheet from ABB [20], [21].

This paper is organized as follows. Section II depicts system configuration and control mechanism. Simulation results are presented in Section III and Section IV gives the conclusion.

System configuration and control mechanism

For high power application condition, such as data center, medical center and so on, a higher power stress is put on the both AC/DC and DC/AC in conventional online UPS system. With the modular online UPS system as shown in Fig. 1(a), power rate of the inverter stage is reduced by using numbers of DC/AC modules, which is a cost-effective, flexibility-effective issue.

A. System configuration

For single DC/AC modules, conventional 3-phase half bridge is considered as shown in Fig. 1(b). The detailed information is presented in Table I. AC/DC, as another important element in the online UPS system, should be also taken into consideration. Numbers of topologies, such as NPC, 3-phase half-

bridge, have been proposed. Control is achieved in DQ frame, which is illustrated detailed in [22]. Hereby, the analysis doesn't concentrates on the issues of AC/DC control.

Table I: Module Characteristics

Rated Power	200kW
Switching frequency	5kHz
DC bus voltage	760V
Rated output voltage	325V(peak)
Rated output current	410A(peak)
Filter inductance	1.8mH
Filter Capacitance	27μF

B. Control Mechanism

Hereby, a two level controller based on CAN bus network is proposed in order to achieve equal power sharing among modules and UPS system output voltage recovery as shown in Fig. 2(a). The inner loop of each DC/AC module is carried out in $\alpha\beta$ frame with two typical PR controllers for voltage and current loop,

$$G_v(s) = k_{pv} + k_{rv}s/(s^2 + \omega_o^2) \tag{1}$$

$$G_c(s) = k_{pc} + k_{rc}s/(s^2 + \omega_o^2) \tag{2}$$

with k_{pv}, k_{rv}, k_{pc}, k_{rc} and ω_o being the voltage proportional term, voltage resonant term, current proportional term, current resonant term and fundamental frequency respectively. By calculating reactive power 3 phase respectively, each DC/AC module phase signals are modified until they reach the same value, which will contribute to reactive power sharing. On the other hand, a virtual resistor is added into the control loop to achieve active power sharing,

$$\delta_{nk} = \delta_{nkref} - k_{ph}Q_{nk} \tag{3}$$

$$v_{nk} = v_{nkref} - i_{Labc}R_{vir} \tag{4}$$

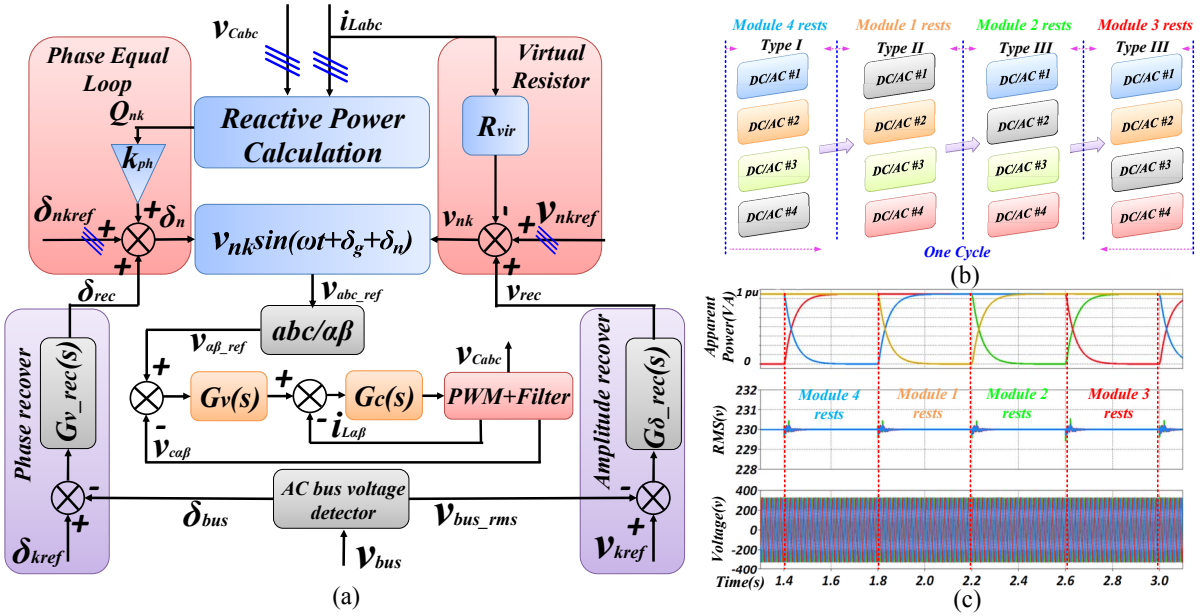

Fig. 2: (a) Overall control diagram; (b) "*heat cycle*" mechanism; (c) "*heat cycle*" simulation.

Here n is the module number (1,2,3…N), k is the phase order (a, b, c), V_{nkref} is the nominal voltage reference, R_{vir} is the virtual resistor, δ_{nkref} is the nominal phase reference, k_{ph} is the phase regulating coefficients and Q_{nk} is the reactive power of each phase of each DC/AC module. Additionally, two typical *PI*s are used to calculate the compensate value for voltage amplitude and phase,

$$G_{v\_rec}(s) = k_{pv\_rec} + k_{iv\_rec}/s \tag{5}$$

$$G_{\delta\_rec}(s) = k_{p\delta\_rec} + k_{i\delta\_rec}/s \tag{6}$$

with k_{pv_rec}, k_{iv_rec}, $k_{p\delta\_rec}$, $k_{i\delta\_rec}$ being voltage amplitude recovery proportional term, voltage amplitude recover integral term, phase recover proportional term and phase recover integral term respectively.

In order to balance the power stress of the each DC/AC module, the four modules are ordered to operate in a circular way, which is called "*heat cycle*", as shown in Fig. 2(b). For instance, when the "*heat cycle*" starts, Module #4 will stop to rest first. Then Module #1 to #3 will stop to rest in turns. Based on this rules, three types of circulating current condition can be defined and studied. It is assumed that all four modules are working together at first. Then, the "*heat cycle*" starts. Firstly, Module #4 rests, while the remaining three modules PWMs are kept synchronized and small balanced currents exist (*Type I*). After that Module #1 rests, while Module #4 starts, which means that Module #2 and #3 PWMs are kept synchronized except Module #4 (*Type II*). Then, Module #2 stops and all the three modules PWMs are not synchronized with each other (*Type III*). At that moment all the modules suffer strong circulating current. Since then, all the modules are ordered to work in turns, and their PWMs are in a similar way. Type III can be considered as a random unsynchronized PWM signal condition. So it happens the most frequently in the real application, which should be paid specific attention. Simulation has been proposed in PLECS to validate the control algorithm. Fig. 2(c) shows the simulation results with four modules operating in a circular way. It can be seen that with modules switching, smaller AC bus voltage oscillation occurred. In order to fast the simulation, the "*heat cycle*" period is chosen to be 0.2***s***, which is much smaller than in the real application.

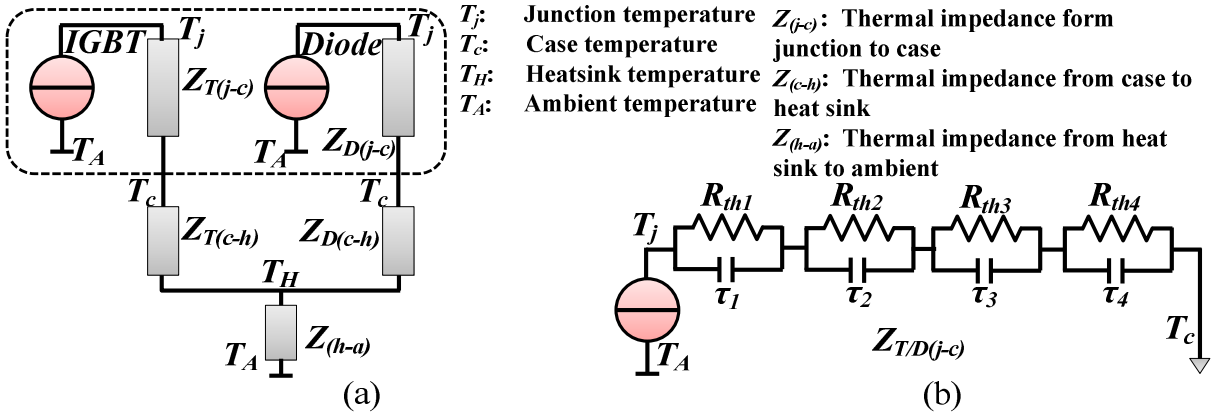

Fig. 3: (a) power devices thermal model; (b) RC network of $Z_{T/D(j-c)}$.

Thermal analysis results

Since thermal conditions of devices are tightly related with the reliability and cooling costs of not only the module itself but also the whole system, it is an important issue, especially in high power applications. In order to obtain accurate loss and temperature date, a proper model should be acquired first. Hereby, the thermal impedance from junction-to-case $Z_{(j-c)}$ is able to be modeled as a four layer *RC* network (see Fig. 3), whose information can be found in the manufacturer datasheet of the device. Since the thermal capacitance is mainly related with dynamic process before reaching steady state [19], the big thermal capacitance of $Z_{T/D(c-h)}$ and $Z_{(h-a)}$ can be neglected in order to achieve a faster simulation.

Based on the module information shown in Table I, IGBT pack 5SND-0800M170100 from ABB is chosen as the switching power devices. The thermal parameters for the devices are listed in Table II. In PLECS, the devices junction temperatures are monitored. Due to the proposed "*heat cycle*" control, there are always three DC/AC modules supporting the load. As a result, the circulating current has to be evaluated in the remaining operating three modules. Normally, UPS modules are designated to work in the load conditions from 50% to 75% [23]. Thus in the simulation, load conditions from 50% to 100% are tested. Here, one leg of the DC/AC (see Fig. 1(b)) is considered because separated heat sink is used for each leg in high power application. The sum of three-phase currents is used to represent the circulating current that each module suffers from [11]. Temperature and loss comparison are performed in switches and diodes respectively. T_1, T_2, D_1 and D_2 (shown in Fig. 1(b)) are analyzed in simulation.

Table II: Parameters of Thermal impedance.

Thermal impedance	$Z_{T/D(j-c)}$			
	1	2	3	4
R_{iIGBT}(K/kW)	15.2	3.6	1.49	0.74
τ_{iIGBT}(ms)	202	20.3	2.01	0.52
R_{iDiode}(K/kW)	25.3	5.78	2.6	2.52
τ_{iIGBT}(ms)	210	29.6	7.01	1.49

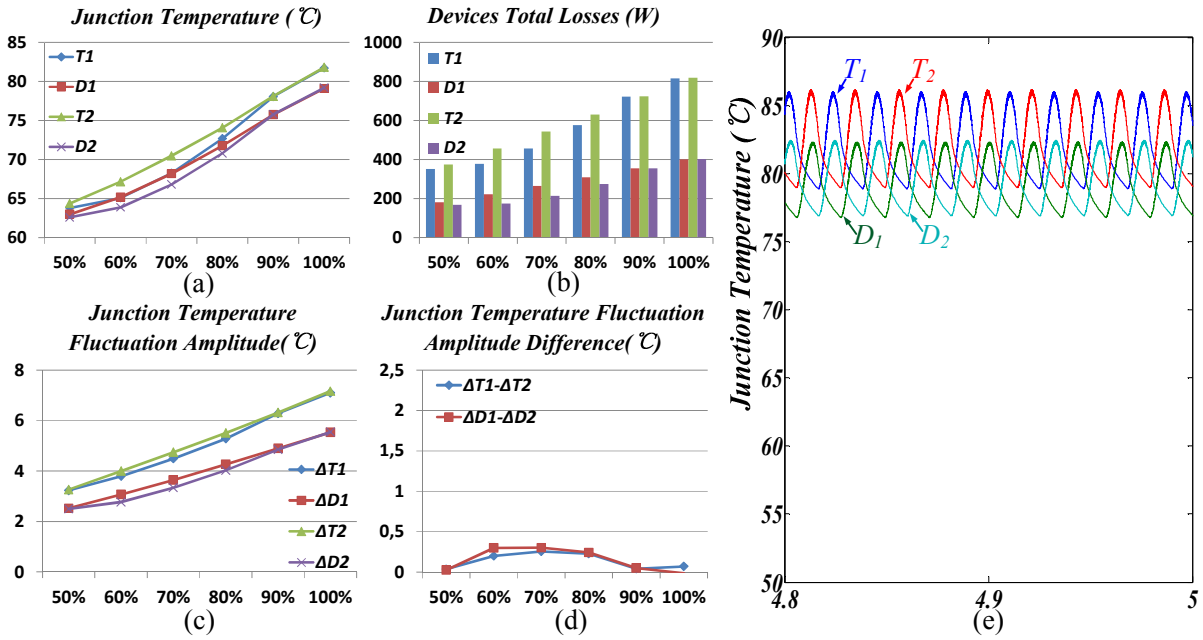

Fig. 4: (a) devices junction temperature; (b) devices total losses; (c) devices temperature fluctuation amplitude; (d) Difference between T_1 and T_2, D_1 and D_2; (e) Temperature details at 100% load condition.

A. *Single DC/AC module*

One single DC/AC module was tested from 50% load to 100% load condition. Fig. 4(a) and (b) show the devices junction temperature and total losses. It can be observed that temperature and losses are distributed almost balanced between T_1 and T_2, D_1 and D_2. Another important factor that needs to pay more attention is the temperature fluctuation amplitude, which is shown in Fig. 4(c) and (d). It can be seen that T_1 and T_2, D_1 and D_2 share similar temperature fluctuation amplitude. Temperature detail at 100% load condition is presented in Fig. 4(e).

B. *Type I*

Hereby, the remaining three modules are tightly synchronized and conventional zero sequence circulating current suppression control method in [11] is used. So each DC/AC module suffers a balanced, similar circulating current. In Fig. 5(a)-(c), it can be observed that the remaining three modules share the same losses distribution condition. T_2 has higher losses than T_1 while D_1 has higher losses than D_2. Moreover, the temperature situation is similar as shown in Fig. 5(d).

As for the temperature fluctuation amplitude, it is presented in Fig. 5(e). T_2 has the highest fluctuation amplitude and it increases suddenly at 90% load condition. Then the amplitude starts to decrease, which is shown in Fig. 5(e). In Fig. 5(f), the fluctuation amplitude difference between T_1 and T_2, D_1 and D_2 is presented. Diodes have a smooth dynamic performance and decrease when the load is changed smaller. The fluctuation amplitude difference between T_1 and T_2, D_1 and D_2 increases suddenly at 90% load condition and then starts to decrease. Three modules temperature information with 100% load is presented in Fig. 5(g)-(i). It can be concluded that three modules shares the same temperature pattern. In real application, PWM will be synchronized or zero sequence circulating current suppression control method will be used in order to avoid such kind of circulating current.

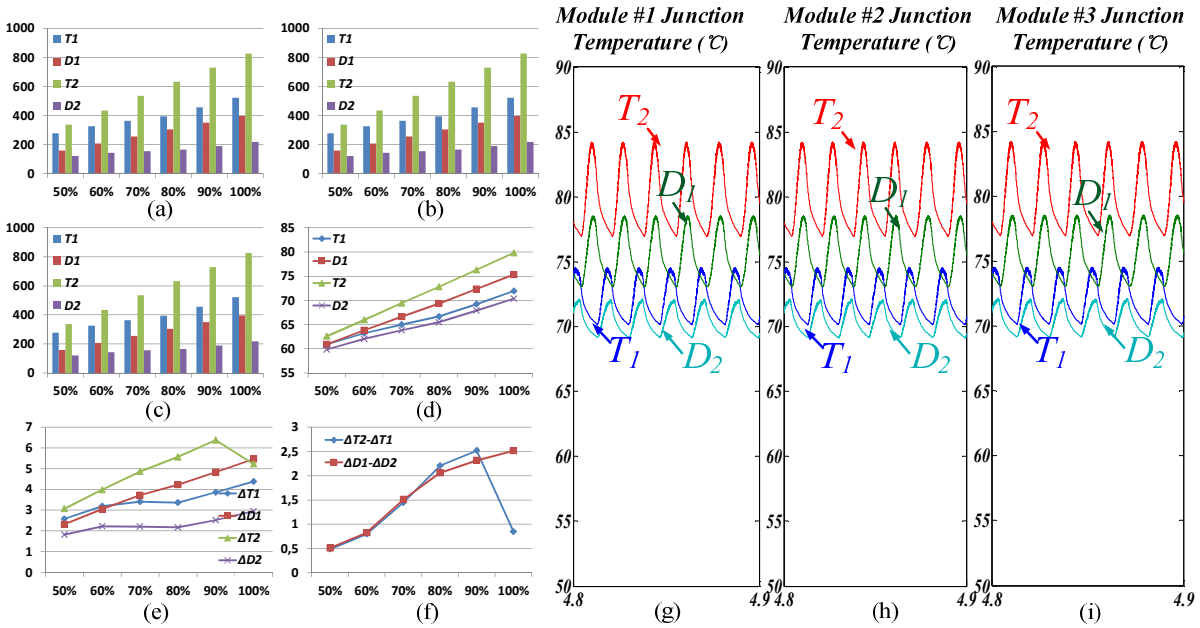

Fig. 5: (a)-(c) loss of module #1, 2 and 3; (d) devices junction temperature; (e) devices temperature fluctuation amplitude; (f) Difference between T_1 and T_2, D_1 and D_2 ; (g)-(i) Temperature details at 100% load condition.

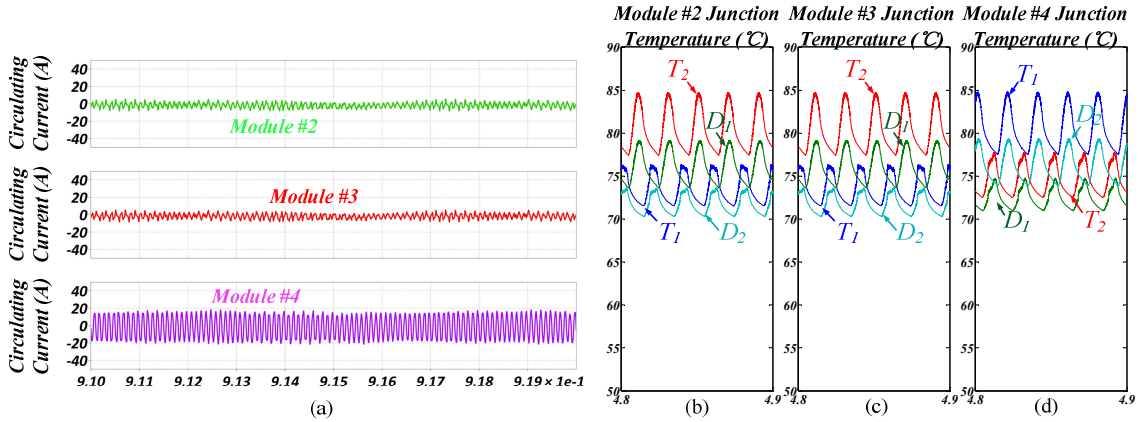

Fig. 6: (a) Circulating current; (b)-(d) Modules detailed temperature at 100% load condition.

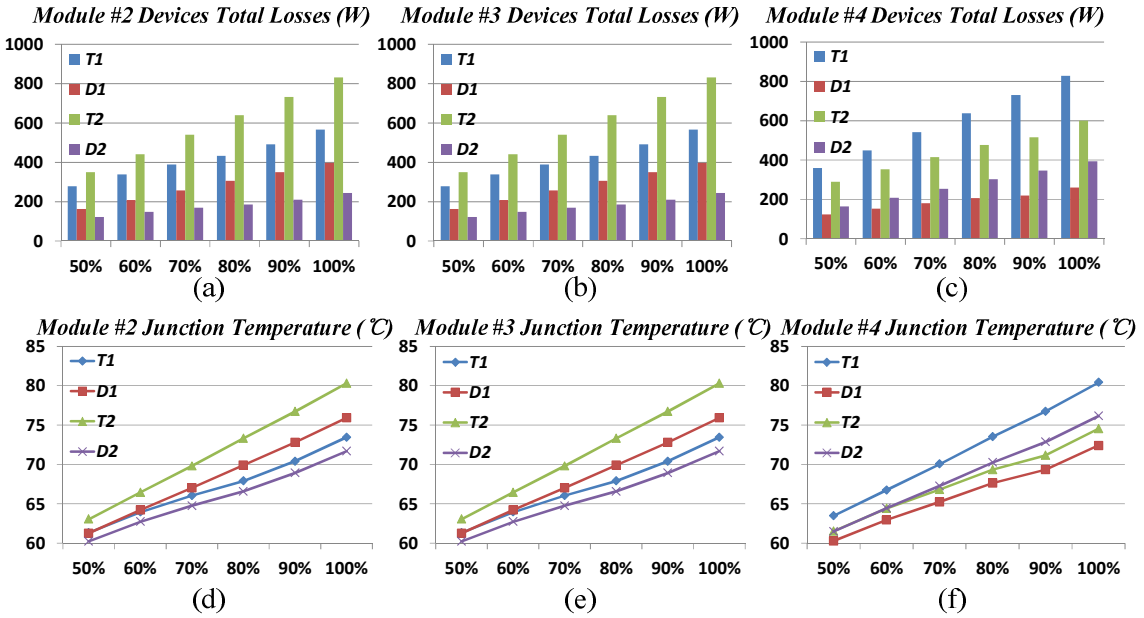

Fig. 7: (a)-(b) loss of module #2, 3 and 4; (d)-(f) devices junction temperature of module #2, 3 and 4.

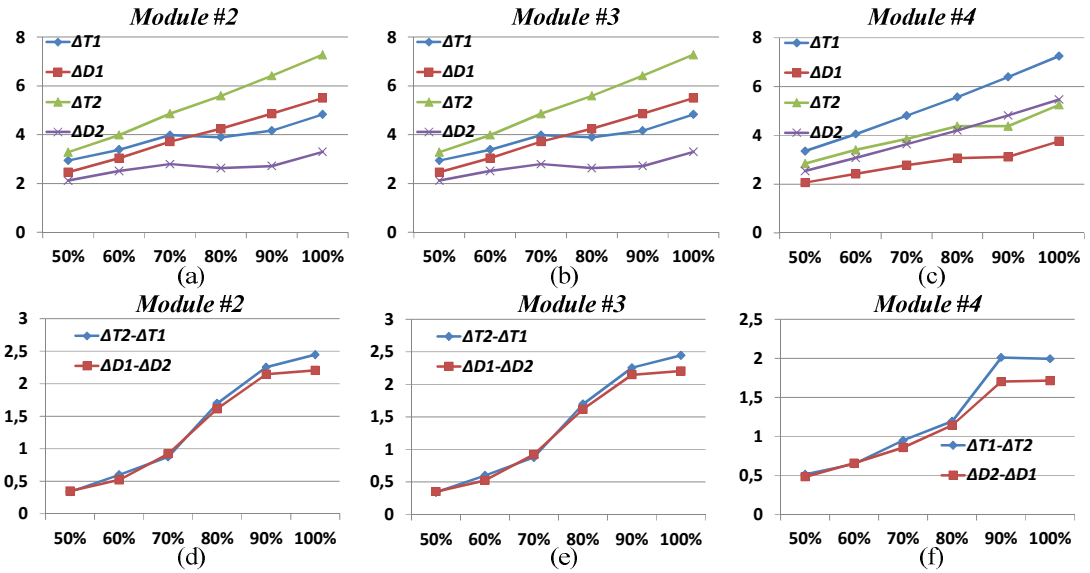

Fig. 8: (a)-(b) temperature fluctuation of module #2, 3 and 4; (d)-(f) temperature fluctuation difference of module #2, 3 and 4.

C. *Type II*

This condition only exists when the system just starts up. Two of the remaining three modules are synchronized and the other module suffers from obvious circulating current (Fig. 6(a) at 100% load condition). It can be seen that module #4 has a different temperature distribution than the other two modules as shown in Fig. 6(b). Through losses calculation (Fig. 7), T_1 in module #4 has higher losses and temperature than T_2 while D_2 in module #4 has higher losses than D_1. In the other two modules, the same temperature and losses patter are shared. T_2 has higher losses and temperature than T_1 while D_1 has higher losses and temperature than D_2.

Fig. 8 depicts the devices temperature fluctuation amplitude of different DC/AC modules. Module #2 and #3 has the same trends which is different from module #4. Due to obvious zero sequence circulating current, the temperature fluctuation amplitude of T_1 is higher than T_2. Similarly, D_2 is higher than D_1. Although different modules have different temperature fluctuation amplitude, the difference between between ΔT_1 and ΔT_2, ΔD_1 and ΔD_1 is decreased with the load becoming smaller as shown in Fig. 8(d)-(f).

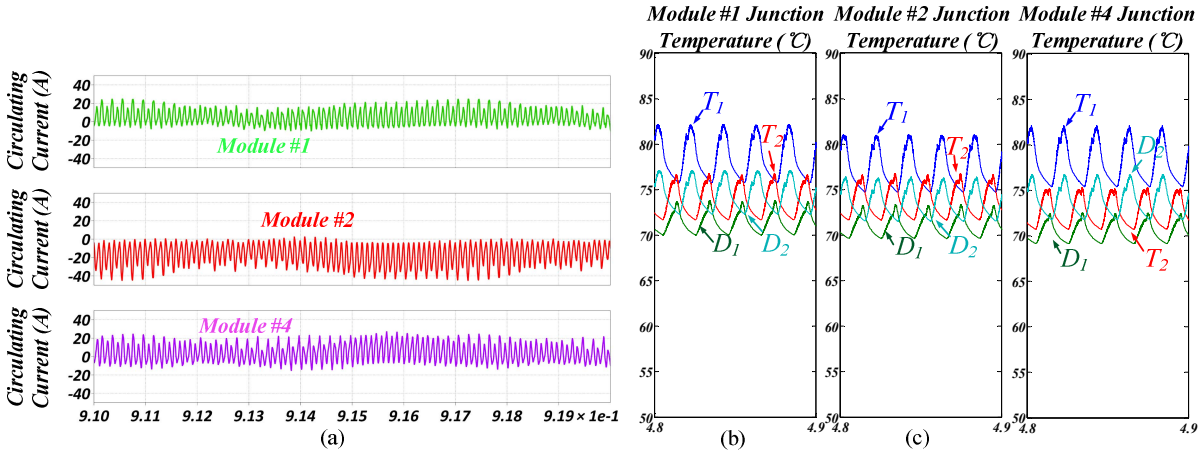

Fig. 9: (a) Circulating current; (b)-(d) Modules detailed temperature at 100% load condition.

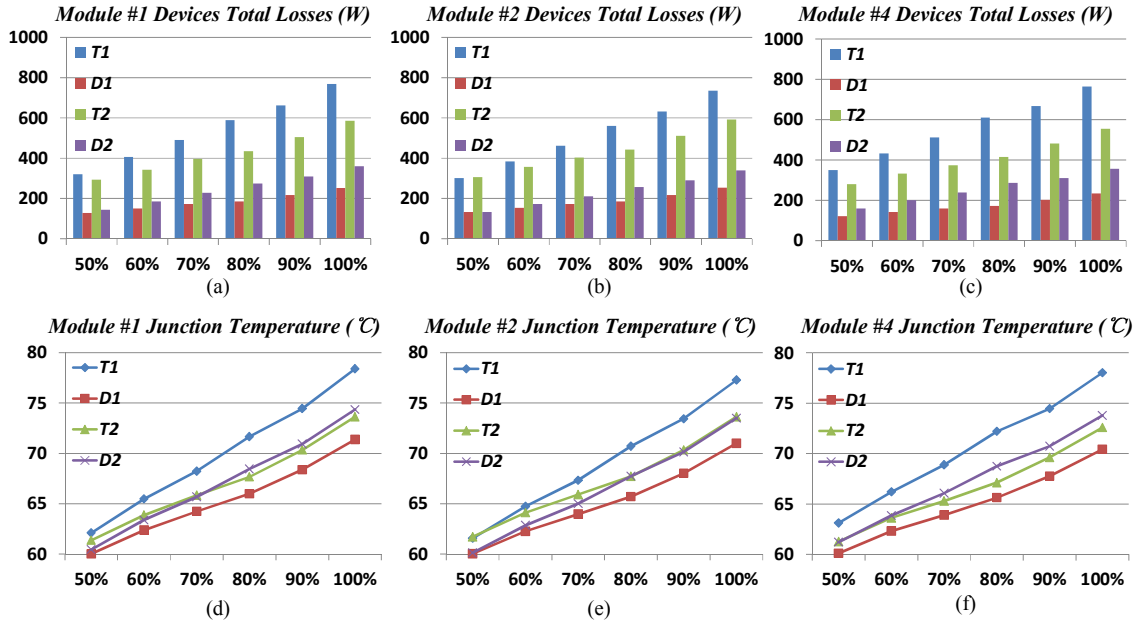

Fig. 10: (a)-(b) loss of module #1, 2 and 4; (d)-(f) devices junction temperature of module #1, 2 and 4.

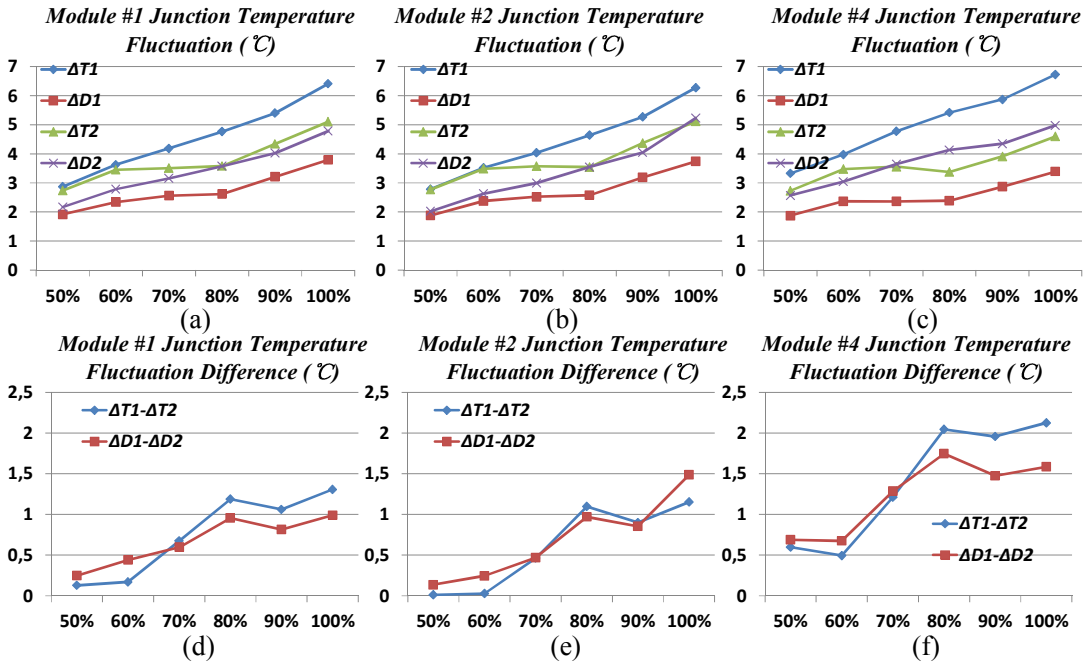

Fig. 11: (a)-(b) temperature fluctuation of module #1, 2 and 4; (d)-(f) temperature fluctuation difference of module #1, 2 and 4.

D. Type III

Since Type *III* occurs the most frequently in the real application, it should be paid specific attention. Fig. 9(a) presents the circulating current condition in Type *III* at 100% load condition. It can be observed that different modules are faced with different circulating current amplitude. And this will cause temperature and losses unbalanced distribution, which is different from type *I* and *II* as shown in Fig. 9(b). In Fig. 10, T_1 has a higher temperature than T_2 while D_2 has a higher temperature than D_1. Moreover, more losses are located on T_1 than T_2. And more losses are observed on D_2 than D_1.

Fig. 11 presents the devices temperature fluctuation amplitude when the load is changing from 50% to 100%. It can be seen that T_1 has higher temperature fluctuation amplitude than T_2 while D_2 has a higher temperature than D_1. However, with the load changing from 100% to 50%, the temperature fluctuation amplitude difference between ΔT_1 and ΔT_2, ΔD_1 and ΔD_1 is becoming smaller except for the 80% load condition. When the load condition is 80%, the temperature fluctuation amplitude difference between ΔT_1 and ΔT_2, ΔD_1 and ΔD_1 suddenly become high and then the difference is becoming smaller again, which is depicted in Fig. 11. Since each module is faced with different circulating current, the temperature distribution situation varies among different modules.

Conclusion

In this paper, thermal and losses distribution is analyzed for different circulating current conditions, namely balanced circulating current (*Type I*) and unbalanced circulating current (*Type II* and *III*). In balanced condition, all modules PWMs are synchronized with each other and suppression control method is considered. In such a kind of suppressed and balanced circulating current conditions, more losses are distributed in T_2 and D_1 of one leg. Higher junction temperature is also observed in T_2 and D_1 .On the other hand, if the modular system suffers from unbalanced circulating current, which happens often in real applications, T_1 and D_2 present more losses and higher junction temperatures.

References

[1] S. Karve,, "Three of a kind [UPS topologies, IEC standard]," IEE Review, vol.46, no.2, pp.27,31, Mar 2000.

[2] R.Strzelecki and G. Benysek, Power Electronics in Smart Electrical Energy Networks. London, U.K.: Springer. 2008.
[3] Z.J. Zhou, X. Zhang, P. Xu; W.X. Shen, "Single-Phase Uninterruptible Power Supply Based on Z-Source Inverter," Industrial Electronics, IEEE Transactions on , vol.55, no.8, pp.2997,3004, Aug. 2008.
[4] C.C. Yeh, M.D. Manjrekar, "A Reconfigurable Uninterruptible Power Supply System for Multiple Power Quality Applications," Power Electronics, IEEE Transactions on, vol.22, no.4, pp.1361, 1372, July 2007.
[5] B. Zhao, Q. Song, W. Liu, Y. Xiao, "Next-Generation Multi-Functional Modular Intelligent UPS System for Smart Grid," Industrial Electronics, IEEE Transactions on, vol.60, no.9, pp.3602,3618, Sept. 2013.
[6] J.K. Park; J.M. Kwon; E.H. Kim, B.H. Kwon, "High-Performance Transformerless Online UPS," Industrial Electronics, IEEE Transactions on, vol.55, no.8, pp.2943,2953, Aug. 2008.
[7] E.K. Sato, M. Kinoshita, Y. Yamamoto, T. Amboh, "Redundant High-Density High-Efficiency Double-Conversion Uninterruptible Power System," Industry Applications, IEEE Transactions on, vol.46, no.4, pp.1525,1533, July-Aug. 2010.
[8] J.W. Dixon, B.T. Ooi, "Series and parallel operation of hysteresis current-controlled PWM rectifiers," Industry Applications, IEEE Transactions on, vol.25, no.4, pp.644, 651, July-Aug. 1989.
[9] Y. Sato, T. Kataoka, "Simplified control strategy to improve AC-input-current waveform of parallel-connected current-type PWM rectifiers," Electric Power Applications, IEE Proceedings - , vol.142, no.4, pp.246, 254, Jul 1995.
[10] S. Fukuda, K. Matsushita, "A control method for parallel-connected multiple inverter systems," Power Electronics and Variable Speed Drives, 1998. Seventh International Conference on (Conf. Publ. No. 456), vol., no., pp.175, 180, 21-23 Sep 1998.
[11] Y. Zhihong, D. Boroyevich, C. Jae-Young, F.C. Lee, "Control of circulating current in two parallel three-phase boost rectifiers," Power Electronics, IEEE Transactions on , vol.17, no.5, pp.609,615, Sep 2002.
[12] Z. Liu, J. Liu, H. Wang, "Output impedance modeling and stability criterion for parallel inverters with average load sharing scheme in AC distributed power system," Applied Power Electronics Conference and Exposition (APEC), 2012 Twenty-Seventh Annual IEEE, vol., no., pp.1921,1926, 5-9 Feb. 2012.
[13] Z. He, Y. Xing, "Distributed Control for UPS Modules in Parallel Operation With RMS Voltage Regulation,"Industrial Electronics, IEEE Transactions on, vol.55, no.8, pp.2860,2869, Aug. 2008.
[14] J.M. Guerrero, L. Garcia de Vicuna, J. Matas, M. Castilla, J. Miret, "A wireless controller to enhance dynamic performance of parallel inverters in distributed generation systems," Power Electronics, IEEE Transactions on, vol.19, no.5, pp.1205,1213, Sept. 2004.
[15] W. Yao, M. Chen, J. Matas, J.M. Guerrero, Z. Qian, "Design and Analysis of the Droop Control Method for Parallel Inverters Considering the Impact of the Complex Impedance on the Power Sharing," Industrial Electronics, IEEE Transactions on, vol.58, no.2, pp.576,588, Feb. 2011.
[16] J.M. Guerrero, J.C. Vasquez, J. Matas, L.G. de Vicuña, M. Castilla, "Hierarchical Control of Droop-Controlled AC and DC Microgrids—A General Approach Toward Standardization," Industrial Electronics, IEEE Transactions on, vol.58, no.1, pp.158,172, Jan. 2011.
[17] J.M. Guerrerol, M. Chandorkar, T. Lee P.C. Loh "Advanced Control Architectures for Intelligent Microgrids—Part I: Decentralized and Hierarchical Control," Industrial Electronics, IEEE Transactions on, vol.60, no.4, pp.1254-1262, April 2013.
[18] TMS320F2833x, 2823x Enhanced Controller Area Network (eCAN) Reference Guide, TEXAS INSTRUMENTS, January 2009.
[19] W. Lixiang, J. McGuire, R.A. Lukaszewski, "Analysis of PWM frequency control to improve the lifetime of PWM inverter," Energy Conversion Congress and Exposition, 2009. ECCE 2009. IEEE , vol., no., pp.900,907, 20-24 Sept. 2009.
[20] ABB Application Note: Applying IGBTs, May 2007.
[21] ABB Hipak, IGBT Module 5SND 0800M170100, Apr 2014.
[22] R. Teodorescu, M. Liserre, P. Rodríguez, "Grid Converters for Photovoltaic and Wind Power Systems. Grid Converters for Photovoltaic and Wind Power Systems, "
[23] SG Series UPS 10-600kVA three phase 400Vac with ultra-high efficiency eBoostTM technology, GE.